

Spectral Rigidity and Geometric Localization of Hopf Bifurcations in Planar Predator–Prey Systems

E. Chan–López^{*1}, A. Martín–Ruiz², and Víctor Castellanos¹

¹*Academic Division of Basic Sciences, Universidad Juárez Autónoma de Tabasco (DACB–UJAT), Mexico.*

²*Institute of Nuclear Sciences, National Autonomous University of Mexico (ICN–UNAM), Mexico.*

March 23, 2026

Abstract

We identify a geometric principle governing the location of Hopf and Bogdanov–Takens bifurcations in planar predator–prey systems. The prey coordinate of any coexistence equilibrium undergoing such a bifurcation lies between consecutive critical points of the prey nullcline.

The mechanism is algebraic. At critical points of the nullcline, the vanishing of its derivative induces constraints on the Jacobian that prevent the spectral conditions required for bifurcation from being satisfied. We refer to this phenomenon as *spectral rigidity*.

The principle is established for three model families and one discrete counterpart with qualitatively different nullcline geometries: a quadratic case (Bazykin model), a cubic case (Holling type IV with harvesting), and a rational case (Crowley–Martin functional response). In each case, the localization follows from explicit parametric characterizations and symbolic reduction.

The analysis extends to discrete-time systems. For a map obtained by forward Euler discretization of the Crowley–Martin model, the Neimark–Sacker bifurcation occurs on the descending branch of the nullcline, providing a continuous–discrete duality governed by the same mechanism.

We conjecture that this localization holds for general smooth prey nullclines, with critical points acting as spectral barriers that organise the bifurcation structure.

Keywords: predator–prey systems, Hopf bifurcation, Bogdanov–Takens bifurcation, Neimark–Sacker bifurcation, prey nullcline, spectral rigidity, geometric localization, Bazykin model, Crowley–Martin functional response, Holling type IV.

MSC 2020: 34C23, 37G15, 92D25, 34C05.

^{*}Corresponding author: eduardo.clopez13@gmail.com

1 Introduction

A fundamental question in the qualitative theory of predator–prey systems concerns the *location* of oscillatory instabilities in state space. The classical answer, due to Rosenzweig and MacArthur [13], is that in systems with a monotone functional response the unique coexistence equilibrium loses stability via a Hopf bifurcation when it crosses the vertex of the prey nullcline—the mechanism underlying the paradox of enrichment [14]. This observation, relating a *geometric* feature of the nullcline to a *spectral* property of the linearization, has proved to be one of the most productive ideas in mathematical ecology.

When the model is enriched by intraspecific predator competition (Bazykin [2]), non-monotone functional responses such as Holling type IV [1, 8, 11], harvesting [3], Allee effects [15, 16], or density-dependent mortality [7], the bifurcation structure becomes considerably richer: multiple coexistence equilibria, Bautin bifurcations, and Bogdanov–Takens points of various codimensions may all appear. In these settings, the interplay between nonlinear functional responses and parameter–dependent feedback mechanisms produces a wide variety of local and global dynamical behaviors, whose organization is typically understood through detailed, model–specific bifurcation analyses.

Despite this apparent complexity, a persistent empirical regularity emerges across these models: *the equilibria at which Hopf or Bogdanov–Takens bifurcation occurs invariably have their prey coordinate lying between consecutive critical points of the prey nullcline*. This phenomenon is observed in models with qualitatively different functional responses and parametrizations, yet it has not, to the best of our knowledge, been identified as the manifestation of a general structural principle.

The central aim of this paper is to show that this regularity is not incidental, but rather reflects a geometric mechanism that constrains the spectrum of the Jacobian at coexistence equilibria. More precisely, we show that the critical structure of the prey nullcline induces algebraic constraints on the Jacobian entries that prevent the eigenvalues from satisfying the spectral conditions required for bifurcation at those points. We refer to this mechanism as *spectral rigidity at critical points*. In this way, the geometry of the nullcline acts as a system of *spectral barriers* that organise the bifurcation diagram.

An important feature of this perspective is that it applies uniformly to both continuous- and discrete-time systems. While Hopf bifurcation in flows is characterized by a vanishing trace and Neimark–Sacker bifurcation in maps by a unit determinant, both phenomena are constrained by the same geometric mechanism. This leads to a natural continuous–discrete duality in the localization of oscillatory instabilities, governed entirely by the monotonicity structure of the prey nullcline.

The purpose of this paper is threefold:

- (i) To establish this *geometric localization principle* rigorously for three model families with qualitatively different nullcline geometries—quadratic, cubic, and rational—through complete parametric characterizations and exhaustive case analyses.
- (ii) To identify the common algebraic mechanism—*spectral rigidity at critical points*—that underpins the localization in every case studied, and which operates uniformly across both continuous and discrete dynamical systems.
- (iii) To formulate a precise conjecture extending the principle to arbitrary smooth prey nullclines, linking the critical structure of the nullcline to the geometric organization of the bifurcation diagram.

1.1 Related work

Hammoum, Sari, and Yadi [7] extended the Rosenzweig–MacArthur graphical stability criterion to a general Gause model with variable predator mortality $d(x, y)$, defining an arc \mathcal{A} of the ascending branch of the prey nullcline along which the Jacobian trace is non-negative and showing that Hopf bifurcation occurs at $\partial\mathcal{A}$. They computed explicit first Lyapunov coefficients for the Bazykin, Cavani–Farkas, and Variable–Territory models. Their framework is effective for determining stability and criticality, but does not yield closed-form expressions for the Hopf locus, does not establish that \mathcal{A} is strictly confined below the nullcline vertex, and requires the functional response to be monotone increasing (hypothesis H2: $p'(x) > 0$, $q'(x) > 0$), thereby excluding the Holling type IV case.

Lu and Huang [12] carried out a detailed bifurcation analysis of Bazykin’s model with Holling II response and predator competition, including degenerate Hopf bifurcation of codimension 2 and focus–type BT bifurcation of codimension 3. Their analysis provides a useful reference point for the richer bifurcation structures that may arise in related models.

For the Holling type IV Leslie system, Li and Xiao [11], Huang et al. [8], Dai and Zhao [5], and Cheng and Zhang [3] carried out progressively refined bifurcation analyses (codimension 2 and 3 BT, Hopf cyclicity, cusp and generalized Hopf points). None of these works addresses the geometric localization question.

1.2 Organization of the paper

The paper is organized as follows. Section 2 introduces the general framework and the notion of nullcline critical structure. Section 3 treats the quadratic case (Bazykin model). Section 4 treats the cubic case (Holling type IV with harvesting). Section 5 treats the rational case (Crowley–Martin). Section 6 extends the principle to discrete–time systems. Section 7 identifies the common algebraic mechanism. Section 8 formulates the general conjecture. Section 9 discusses open problems.

2 General Framework

2.1 The class of models

We consider planar predator–prey systems of the form

$$\dot{x} = f_1(x, y), \quad \dot{y} = f_2(x, y), \quad (1)$$

defined on the closed first quadrant $\overline{\mathbb{R}_+^2} = \{(x, y) \in \mathbb{R}^2 : x \geq 0, y \geq 0\}$, where f_1 and f_2 are smooth functions satisfying the standard ecological assumptions: $f_1(0, y) = 0$, $f_2(x, 0) = 0$ for appropriate boundary conditions, and both axes are invariant.

A *coexistence equilibrium point* (CEP) is a point $P^* = (x^*, y^*) \in \mathbb{R}_+^2$ with $x^*, y^* > 0$ satisfying $f_1(P^*) = f_2(P^*) = 0$.

2.2 The prey nullcline and its polynomial degree

The prey nullcline is the curve $\mathcal{N}_x = \{(x, y) : f_1(x, y) = 0, x > 0\}$. In all standard predator–prey models, this can be written as $y = g(x)$ for a smooth function g defined on a subinterval of $(0, \infty)$.

Definition 1. The *polynomial degree of the prey nullcline* is the degree of g viewed as a polynomial (or rational function reduced to polynomial form) in x , after clearing denominators in the functional response. We denote it $n = \deg(g)$.

Example 2. (a) **Rosenzweig–MacArthur / Bazykin** (Holling type II): $g(x) = \frac{r}{aK}(K - x)(b + x)$, which is quadratic: $n = 2$. One critical point (maximum) at $x_v = (K - b)/2$.

(b) **Holling type IV with harvesting** (Leslie-type): $g(x) = (1 - h_1 - x)(a + x^2)$, which is cubic: $n = 3$. Two critical points (local minimum x_{\min} , local maximum x_{\max}) under appropriate parametric conditions.

(c) **Holling type III**: $g(x)$ is generically cubic or quartic depending on the growth function: $n \geq 3$.

A polynomial g of degree n has at most $n - 1$ critical points in the interior of the ecologically relevant region $\{x : g(x) > 0\}$. These critical points partition this region into at most n subintervals.

2.3 Hopf and Bogdanov–Takens conditions

Let $J(P^*)$ denote the Jacobian of (1) at a CEP P^* . The conditions for bifurcation at P^* are:

$$\text{Hopf: } \operatorname{tr}(J(P^*)) = 0, \quad \det(J(P^*)) > 0, \quad (2)$$

$$\text{Bogdanov–Takens: } \operatorname{tr}(J(P^*)) = 0, \quad \det(J(P^*)) = 0. \quad (3)$$

Both conditions require the trace to vanish. The central observation of this paper is that the trace, evaluated along the prey nullcline, possesses a sign structure that is governed by the critical points of g .

3 The Quadratic Case: Bazykin Model

3.1 Model and nullcline geometry

The Bazykin predator–prey model is

$$\begin{aligned} \dot{x} &= r x \left(1 - \frac{x}{k}\right) - \frac{a x y}{x + b}, \\ \dot{y} &= e \frac{a x y}{x + b} - d y - \sigma y^2, \end{aligned} \quad (4)$$

with all parameters positive. The prey nullcline is the parabola

$$g(x) = \frac{r}{ak} (k - x)(b + x), \quad \deg(g) = 2, \quad (5)$$

with unique critical point (maximum) at $x_v = \frac{1}{2}(k - b)$, requiring $k > b$.

3.2 Localization theorem

Theorem 3 (Quadratic Localization). *Let a be the bifurcation parameter in system (4) with $k > b > 0$. Then every coexistence equilibrium at which a Hopf bifurcation occurs satisfies*

$$0 < x^* < x_v = \frac{k - b}{2}.$$

Proof sketch. We introduce control parameters $k_0 > 0$, $x_0 > 0$ and set $k = k_0 + b + x_0$, which parametrizes the constraint $b - k + 2x < 0$ explicitly. Three cases are analyzed:

Case 1 ($x^* = x_v$): Setting $x = (k - b)/2$ and conditioning e so that this is a CEP, the Jacobian trace evaluates to

$$\text{tr}(J) = -\frac{(k_0 + 2b)^2 r \sigma}{4 a (k_0 + b)} < 0$$

for all admissible parameters. The trace is strictly negative, so the Hopf condition $\text{tr}(J) = 0$ cannot be met.

Case 2 ($x^* > x_v$, descending branch): Parametrizing $x^* = x_v + x_0$ with $x_0 > 0$, both summands of the trace are strictly negative. Again $\text{tr}(J) < 0$ identically.

Case 3 ($x^* < x_v$, ascending branch): The system $\{f_1 = 0, f_2 = 0, \text{tr}(J) = 0, \det(J) > 0\}$ admits solutions with all parameters positive. The critical bifurcation value is

$$a_0 = \frac{(k_0 + 2b)^2 (k_0 + 2b + 2x_0) \sigma}{4 k_0 x_0} > 0,$$

and the equilibrium is

$$P_0 = \left(\frac{k_0}{2}, \frac{k_0 r x_0}{(k_0 + 2b)(k_0 + b + x_0)\sigma} \right)$$

One verifies directly that $\det(J)|_{P_0} = e r x_0 (k_0 + 2b + 2x_0)\sigma / (k_0 + b + x_0) > 0$ for all admissible parameters, so the Hopf condition is fully satisfied at P_0 .

Since Cases 1 and 2 exclude Hopf bifurcation and Case 3 realizes it, the localization is proved. \square

Remark 4. The same case analysis shows that the Bogdanov–Takens condition ($\text{tr}(J) = 0$ and $\det(J) = 0$) is also confined to $x^* < x_v$, since in Cases 1 and 2 the trace cannot vanish regardless of the determinant value.

4 The Cubic Case: Holling Type IV with Harvesting

4.1 Model and nullcline geometry

We consider the Leslie-type system

$$\begin{aligned} \dot{x} &= x(1 - x) - \frac{xy}{a + x^2} - h_1 x, \\ \dot{y} &= y \left(\delta - \frac{\beta y}{x} \right) - h_2 y, \end{aligned} \tag{6}$$

with all parameters non-negative. Introducing $h_{10} > 0$ and setting $h_1 = h_{10}/(3 + h_{10})$, $a = 9/(4(3 + h_{10})^2)$, the prey nullcline becomes a cubic

$$g(x) = -\frac{(h_{10}x + 3x - 3)(9 + 4(3 + h_{10})^2x^2)}{4(3 + h_{10})^3}, \quad \deg(g) = 3, \quad (7)$$

with two critical points:

$$x_{\min} = \frac{1}{2(3 + h_{10})}, \quad x_{\max} = \frac{3}{2(3 + h_{10})}. \quad (8)$$

4.2 Localization theorem

Theorem 5 (Cubic Localization). *In system (6) under the above reparametrization, let β be the bifurcation parameter. Then every coexistence equilibrium at which a Hopf bifurcation occurs satisfies*

$$x_{\min} < x^* < x_{\max}.$$

Proof sketch. The augmented system $\{f_1 = 0, f_2 = 0, \text{tr}(J) = 0\}$ solved for y, δ, β as functions of x yields expressions $y_0(x), \delta_0(x), \beta_0(x)$. A complete symbolic reduction via Reduce in *Mathematica* establishes that

$$y_0 > 0, \quad \delta_0 > 0, \quad \beta_0 > 0, \quad \det(J) > 0 \quad \iff \quad x_{\min} < x < x_{\max}.$$

The boundary cases are verified directly: at $x = x_{\min}$ and $x = x_{\max}$, the solution gives $\beta_0 = 0$ (inadmissible); for $x < x_{\min}$, $\beta_0 < 0$; for $x > x_{\max}$, $y_0 < 0$. \square

4.3 Bogdanov–Takens localization

In the three-equilibrium regime (obtained via a refined parametrization with $a_1 = 1$, $x_0 + a_0 = x_1$), the simultaneous conditions $\text{tr}(J) = 0$ and $\det(J) = 0$ yield two solution branches for (β, h_{10}) as functions of x_0 . Both branches require $h_{10} > 0$, which constrains $x_0 \in (\frac{1}{32}, \frac{9}{32})$. The corresponding equilibrium prey coordinates satisfy $x_{\min} < x^* < x_{\max}$, confirming that the BT localization holds in the cubic case as well.

5 The Rational Case: Crowley–Martin Functional Response

The first two cases involve polynomial prey nullclines ($\deg(g) = 2$ and 3). To test the scope of the localization principle beyond the polynomial setting, we now analyze a model whose prey nullcline is a *rational* function with a single maximum.

5.1 Model and nullcline geometry

The Crowley–Martin predator–prey model [4] is

$$\begin{aligned} \dot{x} &= \rho x \left(1 - \frac{x}{k}\right) - \frac{a x y}{(1 + b x)(1 + c y)}, \\ \dot{y} &= \frac{\gamma a x y}{(1 + b x)(1 + c y)} - d y, \end{aligned} \quad (9)$$

where $c \geq 0$ is the *predator interference parameter*. When $c = 0$, system (9) reduces to the classical Rosenzweig–MacArthur model with Holling type II response $ax/(1+bx)$.

Setting $\dot{x}/x = 0$ and solving for y , the prey nullcline is

$$g(x) = \frac{h(x)}{a - ch(x)}, \quad h(x) := \rho \left(1 - \frac{x}{k}\right) (1 + bx), \quad (10)$$

which is a *rational function* of x (not polynomial for $c > 0$), with a bell-shaped profile vanishing at $x = k$ and $x = 0$ having $g(0) = \rho/(a - c\rho) > 0$ when $a > c\rho$.

The key observation is that

$$g'(x) = \frac{ah'(x)}{(a - ch(x))^2}, \quad (11)$$

so $g'(x) = 0$ if and only if $h'(x) = 0$. The function h is the standard Holling type II nullcline (a parabola), so

$$x_v = \frac{bk - 1}{2b}, \quad (12)$$

which is **independent of the interference parameter** c . The parameter c modulates the height and curvature of the bell but not the location of its peak.

5.2 Localization theorem

Theorem 6 (Crowley–Martin Localization). *In system (9) with $c > 0$ and $bk > 1$, let c be the bifurcation parameter. Then every coexistence equilibrium at which a Hopf bifurcation occurs satisfies*

$$0 < x^* < x_v = \frac{bk - 1}{2b}.$$

Moreover, the critical value of the interference parameter at a Hopf point with prey coordinate x^* is given explicitly by

$$c_0(x) = \frac{abx(k_0 - 2bx)}{d(1+bx)^2(1+k_0-bx)}, \quad (13)$$

where $k_0 = bk - 1$, so that $x_v = k_0/(2b)$. Since all factors in the denominator are positive in the ecologically relevant region, $c_0(x) > 0$ if and only if $k_0 - 2bx > 0$, i.e. $0 < x < x_v$.

Proof. We introduce $k_0 > 0$ via $k = (1 + k_0)/b$ so that $bk - 1 = k_0$ and $x_v = k_0/(2b)$. The Jacobian of (9) at a CEP $(x^*, g(x^*))$ has the trace

$$\text{tr}(J) = \underbrace{\frac{\rho x(bk - 1 - 2bx)}{k(1+bx)}}_{J_{11} \text{ (prey part, independent of } c)} - \underbrace{\frac{dcg(x)}{1+cg(x)}}_{J_{22} \text{ (predator part, } \leq 0)}.$$

A crucial property is that $J_{11}|_{\text{nullcline}}$ depends on x and the prey parameters (ρ, k, b) but *not* on c . This is because the c -dependence in $\partial f_1/\partial x$ cancels exactly when y is substituted from the nullcline relation $\rho(1 - x/k) = ay/((1+bx)(1+cy))$.

At $x = x_v$: $bk - 1 - 2bx_v = 0$ so $J_{11} = 0$ and $\text{tr}(J) = -dcg(x_v)/(1+cg(x_v)) < 0$ for all $c > 0$. Hopf is impossible.

For $x > x_v$: $bk - 1 - 2bx < 0$ so $J_{11} < 0$ and both summands are non-positive. $\text{tr}(J) < 0$. Hopf is impossible.

For $0 < x < x_v$: $J_{11} > 0$. Setting $\text{tr}(J) = 0$ and using the identity $cg(x)/(1+cg(x)) = ch(x)/a$ (which follows from (10)), we obtain (13). All factors are positive, so $c_0 > 0$, and a valid Hopf point exists. \square

Remark 7 (Recovery of the classical Hopf point). As $c \rightarrow 0^+$, formula (13) shows that $c_0(x) \rightarrow 0$ requires $k_0 - 2bx \rightarrow 0$. More precisely, keeping x as a free variable and taking $c \rightarrow 0^+$ in the Hopf condition $\text{tr}(J) = 0$, the unique solution for the prey coordinate satisfying all ecological constraints is $x \rightarrow x_v$. This recovers the classical Rosenzweig–MacArthur result that, in the absence of predator interference, Hopf bifurcation occurs precisely at the vertex of the parabolic prey nullcline. For $c > 0$, the Hopf equilibrium is displaced to the left of the vertex into the ascending branch, with larger c corresponding to smaller x^* .

6 The Discrete Case: Neimark–Sacker Bifurcation in Maps

The preceding sections establish the localization principle for continuous–time systems, where the Hopf condition requires $\text{tr}(J) = 0$ with $\det(J) > 0$. It is natural to ask whether an analogous result holds for discrete-time systems, where the relevant bifurcation—the Neimark–Sacker bifurcation—demands $\det(J) = 1$ with $|\text{tr}(J)| < 2$ [9, 10]. We shall show that it does, and that the mechanism is, in a precise sense, the same.

6.1 The discrete Crowley–Martin model

Consider the discrete predator–prey system (map) with Crowley–Martin functional response:

$$\begin{aligned} x_{n+1} &= x_n + \rho x_n \left(1 - \frac{x_n}{k}\right) - \frac{a x_n y_n}{(1 + b x_n)(1 + c y_n)}, \\ y_{n+1} &= y_n + \frac{\gamma a x_n y_n}{(1 + b x_n)(1 + c y_n)} - d y_n. \end{aligned} \tag{14}$$

This is the forward Euler discretization of the continuous system (9): the map has the structure $x_{n+1} = x_n + F(x_n, y_n)$, where F is the continuous vector field. A fixed point (x^*, y^*) satisfies $F(x^*, y^*) = 0$, which is *precisely* the equilibrium condition of the flow. It follows at once that the prey nullcline of the map—defined by the condition $x_{n+1} = x_n$ with $x > 0$ —coincides with that of the continuous model:

$$\rho \left(1 - \frac{x}{k}\right) = \frac{a y}{(1 + b x)(1 + c y)}, \tag{15}$$

whence $y = g_{\text{map}}(x) = h(x)/(a - ch(x))$ with the same auxiliary function $h(x) = \rho(1 - x/k)(1 + bx)$ as in (10). In particular, the vertex location $x_v = (bk - 1)/(2b)$ is identical to that of the continuous case and is independent of c .

6.2 Spectral rigidity: $J_{00}^{\text{map}} = 1$ at the vertex

Since $f_1^{\text{map}}(x, y) = x + f_1(x, y)$, differentiation with respect to x gives

$$J_{00}^{\text{map}} = 1 + J_{11}^{\text{cont}}, \tag{16}$$

where $J_{11}^{\text{cont}} = \partial f_1 / \partial x$ is the $(1, 1)$ -entry of the Jacobian of the continuous system (9). On the prey nullcline, which is common to both the flow and the map, the simplification of Section 5.2 applies *verbatim*:

$$J_{00}^{\text{map}} \Big|_{\text{nullcline}} = 1 + \frac{\rho x (bk - 1 - 2bx)}{k(1 + bx)} = \frac{k(1 + bx) + \rho x (bk - 1 - 2bx)}{k(1 + bx)}, \quad (17)$$

which is **independent of c** . At $x = x_v = (bk - 1)/(2b)$, the linear factor $bk - 1 - 2bx_v$ vanishes by definition, so

$$\boxed{J_{00}^{\text{map}} \Big|_{x=x_v} = 1 \quad (\text{exactly}).} \quad (18)$$

This is the discrete counterpart of $J_{11}^{\text{cont}} \Big|_{x_v} = 0$:

	At the vertex	Spectral consequence
Flow	$J_{11} = 0$	$\text{tr}(J) = J_{22} < 0$: eigenvalues in left half-plane
Map	$J_{00} = 1$	eigenvalue product constrained away from 1

For $x > x_v$ (descending branch), J_{00} deviates from 1, enabling $\det(J) = 1$ to be achieved for an appropriate bifurcation parameter value.

Theorem 8 (Discrete Localization). *In the discrete Crowley–Martin system (14), the Neimark–Sacker bifurcation at a coexistence fixed point occurs with $x^* > x_v$, i.e. on the descending branch of the prey nullcline. Moreover:*

- (i) *The vertex $x_v = (bk - 1)/(2b)$ is independent of c (same mechanism as in the continuous case: $g'_{\text{map}} = 0 \Leftrightarrow h' = 0$).*
- (ii) *$J_{00}^{\text{map}} = 1$ exactly at x_v , as a direct consequence of the identity (16) and the vanishing of J_{11}^{cont} at the vertex.*
- (iii) *For $x^* > x_v$, the entry J_{00}^{map} deviates from unity, providing the spectral degree of freedom necessary for the Neimark–Sacker condition $\det(J) = 1$ to be realized.*

The essential observation may be stated as follows:

The spectral condition for bifurcation differs between continuous and discrete systems—trace vanishing in the former, unit determinant in the latter—yet the geometric localization remains invariant: it is governed entirely by the critical structure of the prey nullcline.

In both settings, the vertex of the prey nullcline serves as a *spectral boundary*. In flows, it separates the region where $J_{11} > 0$ (ascending branch, Hopf possible) from $J_{11} < 0$ (descending branch, trace irrecoverably negative). In maps, the same vertex separates the region where the determinant can attain unity (descending branch, Neimark–Sacker possible) from where it cannot. The nullcline vertex is, in each case, the organizing center of the local bifurcation structure.

Remark 9 (Continuous–discrete duality). The localization principle exhibits a noteworthy duality: in continuous systems the Hopf bifurcation is confined to the ascending branch ($x^* < x_v$), whereas in discrete systems the Neimark–Sacker bifurcation is confined to the descending branch ($x^* > x_v$). The vertex x_v serves as the common boundary in both cases.

This duality admits a natural spectral interpretation: the Hopf condition $\text{tr}(J) = 0$ with $\det(J) > 0$ constrains the eigenvalue *sum*, while the Neimark–Sacker condition $\det(J) = 1$ with $|\text{tr}(J)| < 2$ constrains the eigenvalue *product*. These complementary constraints, mediated by the same spectral rigidity at the vertex, select opposite sides of the critical point.

7 The Common Mechanism: Spectral Rigidity at Critical Points

The proofs of [Theorems 3, 5, 6](#) and [8](#) share a common algebraic structure that is independent of the particular spectral condition (trace–zero or unit–determinant) and operates at the level of the *spectrum* of the Jacobian. We now isolate this structure and give it a precise formulation.

7.1 From trace rigidity to spectral rigidity

In a continuous-time system, the Hopf condition $\text{tr}(J) = 0$ constrains the *sum* of eigenvalues: $\lambda_1 + \lambda_2 = 0$, requiring them to cross the imaginary axis. In a discrete-time system, the Neimark–Sacker condition $\det(J) = 1$ constrains the *product*: $\lambda_1\lambda_2 = 1$, requiring them to cross the unit circle. Both are spectral conditions—they demand that the eigenvalues of the Jacobian reach a prescribed locus in the complex plane.

The observation that unifies all our results is that *neither* the sum *nor* the product can attain its bifurcation value when the equilibrium sits at a critical point of the prey nullcline. This is not a coincidence of two unrelated mechanisms; it is a single phenomenon: geometric criticality of the nullcline constrains the spectrum of the Jacobian.

Definition 10 (Spectral rigidity). We say that the prey nullcline exhibits *spectral rigidity at a critical point* x_c if, whenever $(x_c, g(x_c))$ is a coexistence equilibrium, the condition $g'(x_c) = 0$ constrains the spectrum of $J(x_c, g(x_c))$ in such a way that the eigenvalues cannot satisfy the bifurcation condition—neither $\lambda_1 + \lambda_2 = 0$ (Hopf) nor $\lambda_1\lambda_2 = 1$ (Neimark–Sacker) nor $\lambda_1 = \lambda_2 = 0$ (Bogdanov–Takens)—for any admissible parameter values.

This definition operates at the level of the full spectrum, not of any particular spectral quantity. It is this generality that allows the same principle to govern both flows and maps.

7.2 The spectral rigidity mechanism

At any CEP $(x^*, g(x^*))$ on the prey nullcline, the Jacobian has the structure

$$J = \begin{pmatrix} J_{11}(x^*) & J_{12}(x^*) \\ J_{21}(x^*) & J_{22}(x^*) \end{pmatrix}, \quad (19)$$

where J_{11} encodes prey self–regulation and J_{22} encodes predator self-regulation. In all models studied:

- (i) J_{11} depends on $g'(x^*)$, and $g'(x_c) = 0$ forces $J_{11}(x_c) = 0$ or drives it to a value that eliminates a degree of freedom.

- (ii) J_{22} has a definite sign (typically ≤ 0) that is independent of the nullcline slope.
- (iii) $J_{12} < 0$ (predation reduces prey growth) and $J_{21} > 0$ (predation increases predator growth).

At a critical point x_c , the eigenvalues are:

$$\lambda_{1,2} = \frac{J_{11}(x_c) + J_{22}(x_c)}{2} \pm \sqrt{\left(\frac{J_{11}(x_c) - J_{22}(x_c)}{2}\right)^2 + J_{12}J_{21}}.$$

With $J_{11}(x_c) = 0$ (or constrained), the trace becomes $\text{tr}(J) = J_{22} < 0$ and the determinant becomes $\det(J) = -J_{12}J_{21} > 0$ (but generically $\neq 1$). The eigenvalues are *locked* into a configuration that cannot reach the imaginary axis (for flows) or the unit circle (for maps).

The essential point is:

At critical points of the prey nullcline (i.e., where $g'(x) = 0$), the Jacobian exhibits spectral rigidity: the constraints imposed by the vanishing of the nullcline derivative eliminate the degrees of freedom required for the eigenvalues to satisfy the bifurcation conditions (trace-zero in flows, unit determinant in maps).

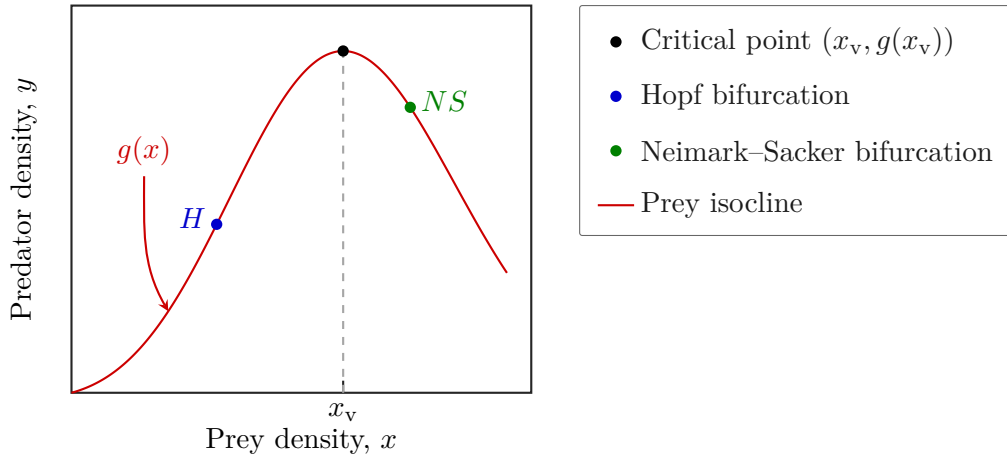


Figure 1: Geometric localization of dynamic instabilities along the prey nullcline defined in (10). The critical point x_v acts as a structural boundary induced by spectral rigidity. In the continuous-time formulation, the Hopf bifurcation is confined to the ascending branch (blue), whereas in discrete-time mappings, the Neimark-Sacker (N-S) bifurcation occurs on the descending branch (green). This geometric separation reflects the continuous-discrete duality of the underlying bifurcation mechanism.

7.3 Verification across all models

We now summarise how the spectral rigidity mechanism manifests in each of the models treated above.

Bazykin (Section 3). At x_v , $J_{11} = 0$ and $J_{22} = -\sigma y^* < 0$, whence $\text{tr}(J) = -\sigma y^* < 0$. The eigenvalues are confined to the open left half-plane.

Holling type IV (Section 4). At x_{\min} and x_{\max} , the Hopf system forces $\beta_0 = 0$, which collapses the predator dynamics. The spectral constraint manifests as the *vanishing of the bifurcation parameter itself*—a particularly rigid form of obstruction.

Crowley–Martin (Section 5). At x_v , $J_{11} = 0$ independently of c , while $J_{22} = -dcy^*/(1 + cy^*) < 0$ for all $c > 0$. The spectrum is rigid for *every* value of the bifurcation parameter simultaneously.

Discrete Crowley–Martin (Section 6). The identity $J_{00}^{\text{map}} = 1 + J_{11}^{\text{cont}}$ transfers the nullcline criticality to the map Jacobian: at x_v , $J_{00}^{\text{map}} = 1$ exactly, and the determinant is constrained away from unity, preventing the eigenvalues from reaching the unit circle.

7.4 Propagation beyond the critical points

Spectral rigidity at the critical points propagates to the exterior of the inter-critical interval by two complementary mechanisms.

In flows (ascending \rightarrow descending). For $x > x_v$ (or outside (x_{\min}, x_{\max}) in the cubic case), J_{11} acquires a definite negative sign that reinforces the negativity of J_{22} . The trace is therefore strictly negative, and the eigenvalues remain in the open left half-plane.

In maps (descending \rightarrow ascending). The discrete structure reverses the role of the branches, but the spectral obstruction persists: on the ascending side of the vertex, the determinant cannot attain unity.

This two-step pattern—*rigidity at the critical point, propagation to the boundary*—constitutes the mechanism behind the geometric localization of bifurcations of periodic orbits in predator–prey systems.

7.5 The deeper principle

The spectral rigidity mechanism reveals a relationship that, while natural in hindsight, is not at all obvious *a priori*:

The geometry of the prey nullcline controls the spectrum of the Jacobian, not the reverse.

In a general dynamical system the spectrum of the Jacobian at an equilibrium depends on all model parameters, and there is no intrinsic reason why a geometric feature of one nullcline should constrain the eigenvalues. The constraint arises because the equilibrium lies on *both* nullclines simultaneously, and the critical structure of the prey nullcline imposes a compatibility condition on the Jacobian entries that propagates to the full spectrum.

In the language of bifurcation theory, the critical points of the prey nullcline are *spectral organizing centers*: they partition the state space into regions of qualitatively distinct spectral behavior, with bifurcations of periodic orbits confined to the transitions between these regions.

8 The General Conjecture

The results of Sections 3 to 6 and the mechanism identified in Section 7 motivate the following conjecture.

Conjecture 11 (Geometric localization of Hopf and Bogdanov–Takens bifurcations). *Consider a smooth (C^2 at least) predator–prey system of the form (1) in the first quadrant of \mathbb{R}^2 , whose prey nullcline $y = g(x)$ possesses exactly two critical points in $(0, \infty)$: a local minimum at x_{\min} and a local maximum at x_{\max} , with $0 < x_{\min} < x_{\max}$. Suppose the system admits exactly three coexistence equilibria. Then:*

- (a) Every coexistence equilibrium at which a Hopf or Bogdanov–Takens bifurcation occurs has its prey coordinate in the interval (x_{\min}, x_{\max}) , i.e. in the region where the nullcline is locally increasing ($g'(x^*) > 0$).
- (b) In the discrete-time (map) version of the system, the Neimark–Sacker bifurcation occurs at equilibria satisfying $g'(x^*) < 0$, i.e. on descending branches of the nullcline.

This dichotomy reflects the spectral rigidity principle: at the critical points $g'(x) = 0$, an algebraic dependence among the Jacobian entries precludes the realization of the spectral conditions for bifurcation (trace-zero in flows, unit determinant in maps), thereby confining bifurcations to regions determined by the monotonicity of the nullcline.

Remark 12 (Evidence). The continuous-time assertion is established for quadratic nullclines (Theorem 3), cubic nullclines (Theorem 5), and rational nullclines (Theorem 6). The discrete-time assertion is established in Theorem 8. A general proof, valid for arbitrary smooth nullclines without case-by-case computation, remains open.

Remark 13 (Role of Bogdanov–Takens bifurcation). Including the BT bifurcation in the conjecture is not merely a matter of completeness: the BT point is the codimension-two organizing center from which Hopf and homoclinic bifurcation curves emanate [9, 6]. Were the BT point able to escape the inter-critical interval, the Hopf curve emanating from it could exit the localization region, invalidating part of the conjecture. The confinement of the BT point (Section 4.3) thus ensures the coherence of the entire local bifurcation structure.

Remark 14 (Polynomial degree and bifurcation complexity). For a polynomial prey nullcline of degree n , there are at most $n - 1$ critical points and hence at most $n - 2$ inter-critical open intervals. The conjecture accordingly predicts that the number of potential localization regions for Hopf and BT bifurcations grows as $n - 2$, providing a concrete link between the *algebraic complexity* of the model (as measured by the degree of its polynomial nullcline) and the *geometric complexity* of its bifurcation diagram.

Remark 15 (Relation to [7]). The graphical criterion of Hammoum, Sari, and Yadi [7] identifies an arc \mathcal{A} of the ascending branch along which the trace is non-negative, with Hopf bifurcation at $\partial\mathcal{A}$. Our conjecture may be viewed as asserting that \mathcal{A} is always strictly contained between consecutive critical points of the nullcline—a structural property not established in [7], where \mathcal{A} is determined implicitly by the equation $H(x) = G(x)$ and its endpoints are obtained numerically. Furthermore, the framework of [7] requires monotone functional response (hypothesis H2: $p'(x) > 0$), excluding the Holling type IV case, whereas our conjecture encompasses non-monotone responses.

9 Conclusions and Open Problems

We have established a geometric localization principle for Hopf and Bogdanov–Takens bifurcations in planar predator–prey systems, proving it for four canonical settings—namely: the Bazykin model with quadratic prey nullcline (Theorem 3), the Holling type IV model with cubic prey nullcline (Theorem 5), the Crowley–Martin model with rational prey nullcline (Theorem 6), and the discrete Crowley–Martin map (Theorem 8). The common mechanism—spectral rigidity at the critical points of the prey nullcline, followed by sign

propagation to the exterior—operates uniformly across continuous and discrete systems and suggests a principle of considerable generality ([Conjecture 11](#)).

Several natural questions remain open:

- (i) **A general proof.** Can the spectral rigidity mechanism be established abstractly for arbitrary smooth prey nullclines, without model-specific computation? A natural approach would be to exploit the factorization of the trace along the nullcline as $\text{tr}(J) = h(x) \cdot (H(x) - G(x))$, in the notation of [7], and to analyze the sign of $H - G$ at and beyond the critical points of g .
- (ii) **Higher-degree nullclines.** Models with Holling type III response, multiple Allee effects, or more elaborate functional forms can generate quartic or higher-degree prey nullclines. Does the localization principle hold in each inter-critical interval independently?
- (iii) **Higher-codimension bifurcations.** The models in [8, 15, 16] exhibit Bogdanov–Takens bifurcation of codimension 3 and 4, and degenerate Hopf of codimension up to 5. Is the localization principle respected by these phenomena?
- (iv) **Non-polynomial nullclines.** When the prey nullcline involves exponential or trigonometric growth functions, can the conjecture be extended using the critical points of the smooth nullcline, even in the absence of a polynomial degree?
- (v) **Global bifurcations.** Homoclinic orbits and limit cycle bifurcations are organized by the Bogdanov–Takens point. If the BT point is geometrically localized, what can be inferred about the *spatial extent* of the corresponding homoclinic loop relative to the nullcline geometry?

The spectral rigidity mechanism is consistent with the behavior observed in predator–prey models with alternative mortality structures, such as variable territory formulations. In these systems, despite significant differences in the predator equation, the same geometric pattern appears: the Jacobian entry J_{11} vanishes at the critical points of the prey nullcline and changes sign across them, while J_{22} remains non-positive at coexistence equilibria. Consequently, the trace is negative at the vertex and along the descending branch, preventing Hopf bifurcation outside the ascending region. A rigorous proof of the localization principle for this class of models is not carried out here and constitutes a natural extension of the present work.

This behavior is not accidental, but reflects a structural constraint imposed by the geometry of the prey nullcline. The prey dynamics determine the regions in phase space where the spectral conditions for bifurcation can be satisfied, independently of the specific form of the predator dynamics.

Acknowledgements

E. Chan–López was supported by SECIHTI through the program “Estancias Posdoctorales por México” (CVU 422090). A. Martín–Ruiz acknowledges financial support from UNAM-PAPIIT (project IG100224), UNAM-PAPIME (project PE109226), SECIHTI (project CBF-2025-I-1862), and the Marcos Moshinsky Foundation. The authors thank Jaume Llibre for helpful comments and suggestions.

Ethics declarations

Conflict of interest

The authors declare no conflicts of interest.

Ethical Approval

Not applicable.

References

- [1] J. F. Andrews, A mathematical model for the continuous culture of microorganisms utilizing inhibitory substrates, *Biotechnol. Bioeng.*, **10** (1968), 707–723.
- [2] A. D. Bazykin, *Nonlinear Dynamics of Interacting Populations*, World Scientific, Singapore, 1998.
- [3] L. Cheng and L. Zhang, Bogdanov–Takens bifurcation of a Holling type IV predator–prey model with constant-effort harvesting, *J. Inequal. Appl.*, **2021** (2021), Article 68.
- [4] P. H. Crowley and E. K. Martin, Functional responses and interference within and between year classes of a dragonfly population, *J. North Am. Benthol. Soc.*, **8** (1989), 211–221.
- [5] Y. Dai and Y. Zhao, Hopf cyclicity and global dynamics for a predator–prey system of Leslie type with simplified Holling type IV functional response, *Int. J. Bifurcation Chaos*, **28** (2018), 1850166.
- [6] J. Guckenheimer and P. Holmes, *Nonlinear Oscillations, Dynamical Systems, and Bifurcations of Vector Fields*, Springer, New York, 1983.
- [7] A. Hammoum, T. Sari, and K. Yadi, The Rosenzweig–MacArthur graphical criterion for a predator–prey model with variable mortality rate, *Qual. Theory Dyn. Syst.*, **22** (2023), Article 36.
- [8] J. Huang, X. Xia, X. Zhang, and S. Ruan, Bifurcation of codimension 3 in a predator–prey system of Leslie type with simplified Holling type IV functional response, *Int. J. Bifurcation Chaos*, **26** (2016), 1650034.
- [9] Yu. A. Kuznetsov, *Elements of Applied Bifurcation Theory*, 3rd ed., Springer, New York, 2004.
- [10] Yu. A. Kuznetsov and H. G. E. Meijer, *Numerical Bifurcation Analysis of Maps: From Theory to Software*, Cambridge University Press, Cambridge, 2019.
- [11] Y. Li and D. Xiao, Bifurcations of a predator–prey system of Holling and Leslie types, *Chaos Solitons Fractals*, **34** (2007), 606–620.
- [12] M. Lu and J. Huang, Global analysis in Bazykin’s model with Holling type II functional response and predator competition, *J. Differential Equations*, **280** (2021), 99–138.

- [13] M. L. Rosenzweig and R. H. MacArthur, Graphical representation and stability conditions of predator–prey interactions, *Am. Nat.*, **97** (1963), 209–223.
- [14] M. L. Rosenzweig, Paradox of enrichment: destabilization of exploitation ecosystems in ecological time, *Science*, **171** (1971), 385–387.
- [15] Z. Shang and Y. Qiao, Multiple bifurcations in a predator–prey system of modified Holling and Leslie type with double Allee effect and nonlinear harvesting, *Math. Comput. Simulation*, **205** (2023), 745–764.
- [16] M. Zhang, Z. Li, F. Chen, et al., Bifurcation analysis of a Leslie–Gower predator–prey model with Allee effect on predator and simplified Holling type IV functional response, *Qual. Theory Dyn. Syst.*, **24** (2025), Article 131.